ARMA 18-320

Gas-driven Rapid Fracture Propagation and Gas Outbursts under Unloading Conditions in Coal Seams

Cao, W., Shi, J.Q., Durucan, S., Si, G. and Korre, A.

Department of Earth Science and Engineering, Royal School of Mines, Imperial College London, London, SW7 2AZ, United Kingdom

Copyright 2018 ARMA, American Rock Mechanics Association

This paper was prepared for presentation at the 52nd US Rock Mechanics / Geomechanics Symposium held in Seattle, Washington, USA, 17–20 June 2018. This paper was selected for presentation at the symposium by an ARMA Technical Program Committee based on a technical and critical review of the paper by a minimum of two technical reviewers. The material, as presented, does not necessarily reflect any position of ARMA, its officers, or members. Electronic reproduction, distribution, or storage of any part of this paper for commercial purposes without the written consent of ARMA is prohibited. Permission to reproduce in print is restricted to an abstract of not more than 200 words; illustrations may not be copied. The abstract must contain conspicuous acknowledgement of where and by whom the paper was presented.

ABSTRACT: Coal and gas outbursts have long posed a serious risk to safe and efficient production in coal mines. It is recognised that the coal and gas outbursts are triggered by excavation unloading followed by gas-driven rapid propagation of a system of pre-existing or mining-induced fractures. Gas-filled fractures parallel to a working face are likely to experience opening first, then expansion and rapid propagation stages under unloading conditions. This research aimed to identify the key factors affecting outburst initiation and its temporal evolution during roadway developments. Specifically, the response of pre-set fractures in a coal seam sandwiched between rock layers to roadway development is simulated using a geomechanical model coupled with fracture mechanics for fracture opening and propagation. In addition, kinetic gas desorption and its migration into open fractures is considered. During simulations outburst is deemed to occur when the fracture length exceeds the dimension of a host element. The findings of this research suggests that the simulated coal and gas outburst may be considered as a dynamic gas desorption-driven fracture propagation process. The occurrence of coal and gas outbursts is found to be influenced mainly by the coal properties, fracture attributes, and initial gas pressure and the in situ stress conditions.

1. INTRODUCTION

Coal and gas outbursts during coal mining is a violent dislodgement and ejection of coal as a consequence of sudden release, at a working face, of the internal gas and strain energy (Farmer and Pooley, 1967; Hargraves, 1980; Shepherd *et al*., 1981). In some instances, as much as thousands of cubic metres of methane or carbon dioxide and hundreds of tonnes of fragmented coal mass are emitted from a working face over a period of several minutes. As a consequence, these hazards usually bring about disastrous outcomes, for instance casualties, equipment damage, and even the abandonment of underground structures.

As early as the 1980s, researchers began to recognise that the propagation of microscopic fractures to form macroscopic splitting fractures is a dynamic process in a wide range of phenomena, such as coal and gas outbursts and rock bursts. In rock bursts, a two-stage process characterised by a slow creep deformation, followed by rapid fracturing associated with seismic energy release have been reported (Dyskin and Germanovich, 1993; Linkov, 1996; Rudajev *et al*., 1986). As well as inducing far-field stress disturbances and an excavation damage zone (EDZ) around underground openings (Cao *et al*., 2016; Li *et al*., 2014, 2016), the release of confining stress at an excavation face also gives rise to some penny-shaped micro-fractures near the opening surface. These mining-induced fractures usually run subparallel to the excavation face (Dyskin and Germanovich, 1993). Such a dominant fracture orientation was also confirmed in laboratory experiments where outbursts could be simulated if the stress was relieved considerably on the front plate of a true-triaxial loading system before unloading, but outburst did not occur if the side plates were largely de-stressed in advance (Alekseev *et al*., 1980).

During coal production, micro fractures grow in the direction perpendicular to the minor principal stress, driven by the gas pressure build up inside the fractures as a result of gas desorption and migration (Anders *et al*., 2014). Gas desorption, which is capable of providing high energy for transporting coal particles over a certain distance, has been reported to be a key factor leading to coal and gas outbursts (Farmer and Pooley, 1967; Feldman *et al*., 2017; Odintsev, 1997; Zhao *et al*., 2016).

Theoretical models combining rock mechanics, fracture mechanics and gas dynamics have been developed to better understand coal and gas outbursts (Chen, 2011; Feldman *et al*., 2017; Odintsev, 1997). Chen (2011) considered the formation of a group of parallel fractures

ahead of a mining face, whose length variation depends on the difference between face advance rate and fracture propagation speed. Using a theoretical model with a main fracture oriented parallel to the working face, Feldman *et al*. (2017) adopted Griffith's criterion to examine the fracture evolution under the combined action of instantaneous unloading and gas filtration to the fracture in coal mines.

Previous work on coal and gas outburst in coal mines has been mainly concerned with the conditions for its initiation. This work aims to obtain a better understanding regarding the temporal evolution of coal and gas outbursts, and identify key parameters contributing to coal and gas outbursts in terms of both potential and intensity. Specifically, the occurrence of coal and gas outbursts when development headings approach towards an outburst prone zone is considered using the developed modelling methodology. The simulated temporal evolution of coal and gas outbursts in terms of ejected volume of coal, stress and gas pressure, and fracture growth are presented, and the key characteristics of coal and gas outbursts associated with coal properties and geological conditions are identified and discussed.

2. THEORETICAL FORMULATION OF A MINING-INDUCED GAS-DRIVEN OUTBURST MODEL

In this section a theoretical model for dynamic (discrete) fracture behaviour ahead of a working face subjected to the interplay of gas pressure and unloading stress conditions is developed to study the onset and evolution of coal and gas outbursts during coal mining. The following requirements should be fulfilled to form a coal and gas outburst as a dynamic domino effect-type phenomenon: (1) fracture propagation is rapid so that a coal fragment can be separated from the coal seam in a very short time, and (2) fragmentation of coal materials as a result of fracture propagation provides conditions for propagation of subsequent exposed fractures. As a first step, the behaviour of a disk-shaped fracture close to a free face, in terms of its opening, subsequent expansion and rapid propagation, under unloading conditions is considered. Fracture mechanics and gas adsorption kinetics are employed to account for fracture propagation and gas desorption behaviours, respectively.

2.1. Conceptual Model

Fig. 1 shows a schematic of a coal seam with a working face and an induced failure zone ahead of the face, and the resulting stress redistribution. In addition, fractures oriented parallel to the advancing face are also created near the face. Fractures are assumed to be penny-shaped, which was confirmed to match field observations in a previous numerical modelling study (Cao *et al*., 2017). Here, the focus is on a newly formed fracture (which is initially closed), and its subsequent opening and propagation as the face advances (Fig. 1). The fracture is subjected to an internal pore pressure p as well as the external stress (the minimum principal stress σ_{min}). The dynamic fracture behaviour is controlled by the effective stress ($\sigma_{eff} = p-\sigma_{min}$).

The intra-fracture gas pressure is affected by the fracture opening (aperture) and inward gas migration. The latter tends to offset the pressure reduction caused by fracture volume increase. In this work, it is assumed that the gas inflow is predominantly the result of gas desorption from the surrounding coals.

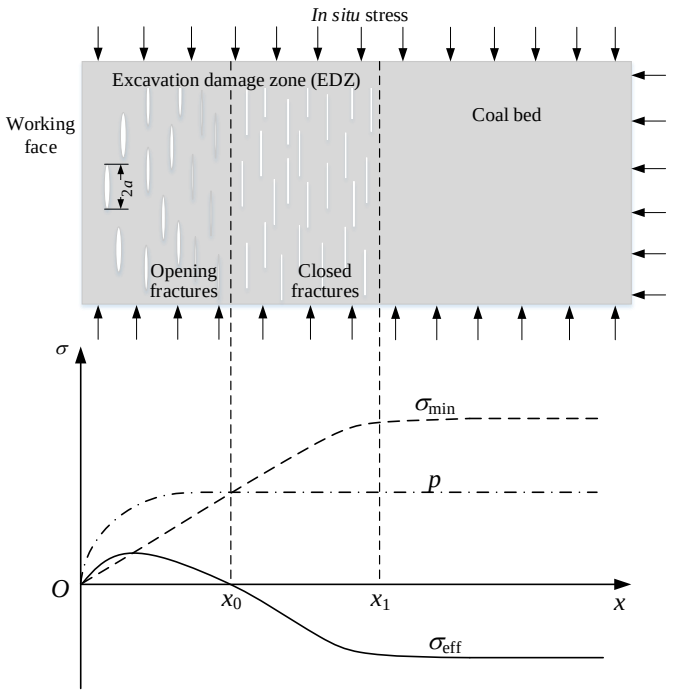

Fig. 1. Schematic representation of fracture opening in relation to effective stress changes ahead of a working face (modified after Feldman *et al.*, 2017).

2.2. Fracture Behaviour Subjected to Intra-Fracture Effective Stress

As shown in Fig. 1, the minimum principal stress acting on the fracture decreases as the face advances towards it. Therefore, the effective stress increases correspondingly, becoming positive eventually. Considering that there is a time-lag in the seam gas pressure response to face advance, the model developed assumes that the initial fracture pressure is equal to the initial seam gas pressure. As the working face advances, the fracture is likely to experience opening first, then expansion and rapid propagation under the interplay of gas pressure and stress. Subscripts for relevant parameters such as fracture radius, fracture volume, intra-fracture gas pressure, etc., are assigned according to evolutional stages, where 0 stands for initial values, 1 for values at the opening and expansion stages, and 2 for values in the propagation stage.

(1) Fracture opening triggered by excavation unloading.

The volume of the induced penny-shaped fracture of radius a and thickness d is given by:

$$V_c = \pi a^2 d \tag{1}$$

The fracture volume as a function of the prevailing effective stress can be obtained by considering the work done by the prevailing effective stress. The total work W done to form a disk-shaped fracture in solid under three-dimensional (3D) stress conditions is given by (Sneddon, 1946):

$$W = \frac{8(1-\mu^2)\sigma_{\text{eff}}^2 a^3}{3E} \tag{2}$$

where μ and E are the Poison's ratio and the Young's Modulus of coal respectively.

The work done is equal to half the integral of the product of the traction over the whole fracture surface and the displacement (Sack, 1946):

$$W = \pi a^2 \sigma_{\text{eff}} d / 2 \tag{3}$$

Combining Eqs. (1), (2) and (3), the volume of an isolated fracture embedded in a coal seam can be written as (Odintsev, 1997):

$$V_c = \frac{16(1-\mu^2)a_0^3 \sigma_{\text{eff},0}}{3E} \tag{4}$$

(2) Gas desorption and its migration into the fracture.

Fracture opening results in an initial decrease in the fracture gas pressure, which prompts the desorption of gas from the coal surrounding the fracture and its subsequent migration to the fracture. The volume of the surrounding coal contributing to gas desorption is given by (Odintsev, 1997):

$$V_{\text{coal}} = 2\pi a_1^2 h \tag{5}$$

where h is the thickness of a loosened surficial microlayer with gas-containing micro-pores on each side of the fracture.

The initial volume of adsorbed gas at pressure P is

$$V_{\text{total}} = \rho V_{\text{coal}} V \tag{6}$$

where V is the adsorbed gas volume per unit mass of coal at pressure P.

According to gas adsorption kinetics, the volume of desorbed gas V_g, following a sudden drop in the gas pressure from p to atmospheric pressure p_{atm} is written as (Crank, 1979):

$$\frac{V_g}{V_{\text{total}}} = 1 - \frac{6}{\pi^2}\sum_{n=1}^{\infty}\frac{e^{-n^2\pi^2\kappa t}}{n^2} \tag{7}$$

where t is the gas desorption time, and κ is the diffusivity of coal which is associated with diffusion coefficient and coal particle radius. For a small gas desorption time, which is the case in the context of this research, the equation has an asymptotic approximation (Smith and Williams, 1984):

$$\frac{V_g}{V_{\text{total}}} = 6\sqrt{\frac{\kappa t}{\pi}} \tag{8}$$

The total volume of gas that can be desorbed due to the change in gas pressure is limited by the Langmuir isotherm given by (Langmuir, 1918):

$$V = \frac{V_L P}{P_L + P} \tag{9}$$

where V is the adsorbed gas volume per unit mass of coal at pressure P, V_L is the Langmuir volume, which is the monolayer volumetric adsorption capacity per unit mass of coal, and P_L is the Langmuir pressure, referred to as the pressure at which half of the Langmuir volume is adsorbed.

The resulting gas pressure p_1 in the fracture with volume V_c is related to V_g by the ideal gas law

$$V_c p_1 = V_g p_{\text{atm}} \tag{10}$$

Meanwhile, V_c is also a function of the gas pressure following Eq. (4)

$$V_c = \frac{16(1-\mu^2)a_1^3(p_1 - \sigma_{\min})}{3E} \tag{11}$$

Substituting Eqs. (8) and (11) in (10) yields the gas pressure p_1 in the fracture.

(3) Fracture propagation.

Based on linear elastic fracture mechanics (LEFM), the material is deemed to fail when the stress intensity factor at a fracture tip, either for mode I (opening mode, K_I) or mode II (sliding mode, K_{II}), reaches a critical value K_{Ic} or K_{IIc}. K_{II} would be zero when there are no free surfaces; otherwise, the interaction between the fracture and the free surface gives rise to a finite K_{II}. However, the stress intensity factor for the mode II (K_{II}) at the tip of a fracture adjacent to a free surface, which is the case in this work, is considerably smaller than that for the mode I (K_I) (Dyskin and Germanovich, 1993). This allows using the stress intensity factor criterion only for the mode I in the evaluation of fracture propagation:

$$K_I \geq K_{Ic} \tag{12}$$

where K_{Ic} is the fracture toughness of coal.

The stress intensity factor K_I for a fracture embedded in an infinite domain can be expressed in terms of effective stress and fracture radius as:

$$K_{\mathrm{I}} = 2\sigma_{\mathrm{eff}}(a/\pi)^{1/2} \tag{13}$$

During fracture propagation, the following equation holds for an isothermal process according to the ideal gas equation of state:

$$p_1 V_{\mathrm{c1}} = p_2 V_{\mathrm{c2}} = znRT = \text{constant} \tag{14}$$

Fracture propagation propelled by a certain volume of desorbed gas results in an increase in fracture radius and a drop in gas pressure as governed by Eqs. (4) and (14). Substituting Eqs. (4) and (14) in Eq. (13), it can be found that K_{I} monotonically decreases as the gas pressure decreases when $p \geq \sigma_{\mathrm{min}}$, which suggests that the propagation would cease at a state where the following equation is satisfied:

$$K_{\mathrm{I2}} = 2(p_2 - \sigma_{\mathrm{min}})(a_2/\pi)^{1/2} = K_{\mathrm{Ic}} \tag{15}$$

It is noted that gas continues to desorb and flow into the fracture due to the decreased intra-fracture gas pressure after the fracture propagates. On the other hand, as Eq. (15) suggests, the increase in fracture radius aggravates the vulnerability of the fracture by lowering the critical intra-fracture gas pressure that is needed for further propagation. This suggests that, once a fracture begins to propagate, it would keep on propagating, rather than reaching a state of equilibrium under continuous gas desorption conditions.

From then on, gas desorption and fracture propagation occur simultaneously. The intra-fracture gas pressure p_2 decreases towards σ_{min}, and the fracture radius increases until a coal fragment is separated from the coal seam and extruded by the residual gas pressure. Given the same fracture radius, fracture toughness and gas desorption conditions, the fracture closest to the free surface is the least loaded and can reach the fracture propagation criterion the most readily. The coal failure induced by this fracture would then turn the next fracture closest to it to one as the most susceptible to failure. In this way, a relatively small spacing between multiple parallel fractures would lead to successive propagation of fractures and coal expulsion from the coal seam, i.e., a coal and gas outburst.

2.3. Estimation of Outburst Threshold Limits

The threshold limits of coal and gas outbursts can be estimated according to Eqs. (12) and (13) using practical ranges of parameters. Fig. 2 presents critical stress intensity factor K_{I} for fractures associated with different values of fracture toughness K_{Ic}, fracture radius a_0, and effective stress p-σ_{min}. As can be seen, large fracture radius, high effective stress and low fracture toughness have a favourable effect on the potential of coal and gas outbursts. For typical coal properties and effective stresses faced in coal mining, the minimum fracture radius that can trigger unstable failure spans from below 10^{-4} to over 10^{-3} m.

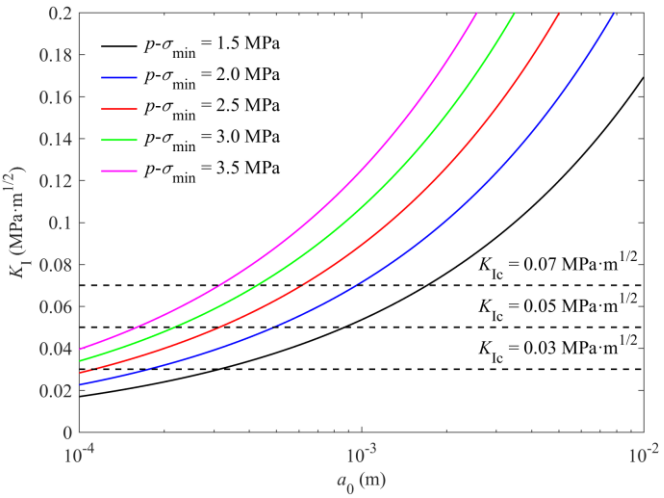

Fig. 2. Stress intensity factor K_{I} as a function of fracture radius a_0 and effective stress p-σ_{min}. Fractures are deemed to propagate if $K_{\mathrm{I}} \geq K_{\mathrm{Ic}}$.

The criterion for coal and gas outbursts can equally be expressed in terms of intra-fracture gas pressure, that is, a fracture with continuous inflow of desorbed gas is deemed to propagate if the critical intra-fracture gas pressure p_{lim} to drive fracture propagation is lower than that at adsorption/desorption equilibrium p_{equ}. As coal and gas outbursts initiate from the working face, it is essential to examine the criterion for fracture propagation at this specific location where the minor principal stress can be approximated as 0. As illustrated in Fig. 3, the intra-fracture gas pressure threshold p_{lim} associated with different values of fracture toughness K_{Ic}, fracture radius a_0 and initial gas pressure p_0 for fractures located close to a working face were calculated using coal seam properties from a Colliery in the Upper Silesian Coal Basin in Poland (later presented in Section 4). Because p_{equ} is dominated by p_0, and is independent of strength properties of coal such as fracture toughness K_{I} or fracture radius a_0, this alternative criterion isolates the impact of initial gas pressure on the potential for coal and gas outbursts.

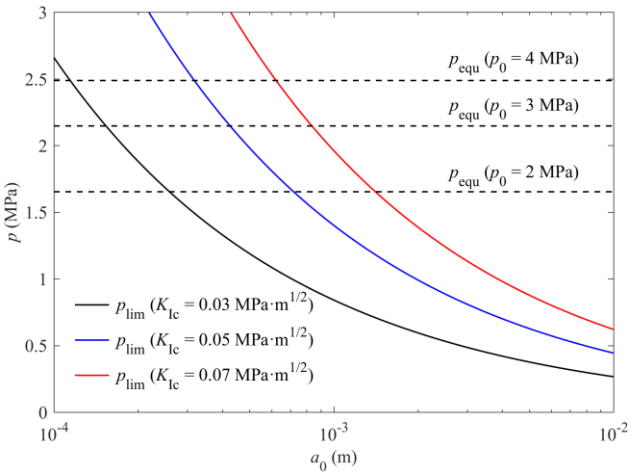

Fig. 3. Intra-fracture gas pressure p_{lim} as a function of fracture toughness K_{Ic} and fracture radius a_0 for fractures located close

to a working face. Fractures are deemed to propagate if $p_{lim} \leq p_{equ}$.

3. NUMERICAL IMPLEMENTATION OF THE OUTBURST MODEL

Based upon the preceding analyses, a methodology incorporating stress changes, gas desorption and fracture propagation was developed to model the initiation and temporal evolution of a coal and gas outburst triggered by coal extraction. Because it is computationally intensive to perform explicit simulation of fracture propagation in field-scale models, each element of coal seam in the model is assumed to host a gas-containing micro-fracture of the same length, and the failure of model elements is governed by the propagated lengths of embedded fractures. The outburst modelling procedure developed involves three main steps as detailed below.

The *model set-up and initialisation* start with the construction of a 3D model representing the coal seam extracted and the surrounding strata in FLAC^{3D}. A system of gas-containing fractures oriented perpendicular to the minor principal stress is distributed uniformly throughout the model domain of the coal seam. The elastic model is used as the constitutive model, and mechanical properties are assigned to the grid blocks representing different rock formations. The boundary and initial conditions are then applied to the model so as to reach an initial equilibrium state.

Next, the *simulation of stress redistribution* step is performed. Progressive coal extraction is simulated by a series of coal excavation steps, each of which typically reflects face advance in one or a few working days. In each step, coal extraction activities are mimicked by "removing" grid elements representing the coal to be extracted or ejected. This is achieved by assigning null mechanical properties to these elements. In this way, the loads previously withstood by the "removed" cells are redistributed to the surrounding cells and a new stress equilibrium is established. The stress equilibrium is considered to be achieved instantly after the removal of elements.

In the final modelling step, *fracture behaviour evaluation and associated failure analysis* is performed. At the end of each time step, a subroutine specially-written for this purpose is invoked to check whether the embedded fracture has been triggered to expand, and even grow, for each model element based upon the prevailing stress states. When the outburst criterion induced by coal extraction is met in a host element, this element is ejected from the coal seam.

Steps 2 and 3 described above are repeated in each coal excavation step until the end of the physical time to be modelled. A flow chart of the modelling procedure is presented in Fig. 4.

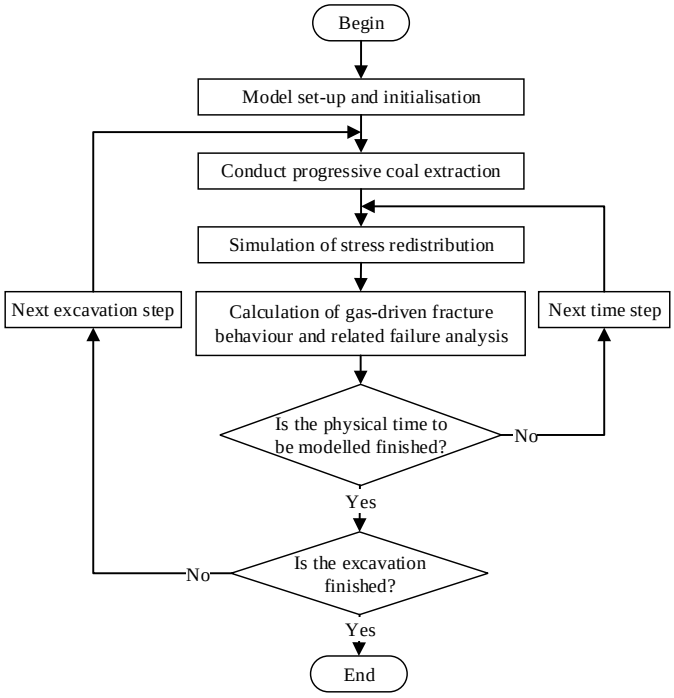

Fig. 4. Flow chart for the modelling procedure.

4. NUMERICAL MODEL SET-UP

The roadway development used as an example to demonstrate the methodology developed in this study utilises the field data and layout from an outburst prone coal seam at a Colliery located in the Upper Silesian Coal Basin in Poland. The coal resource at this Colliery contains multiple stratigraphic layers such as mudstone, sandstone, and aleurolite, etc. and is exploiting a multi-seam deposit using highly efficient longwall mining. The coal seam used for the modelling and assessment of coal and gas outbursts in this research lies at 720 m depth below sea level. A longwall panel measuring around 800 m long and 250 m wide is being developed in the coal seam modelled.

A three-dimensional geomechanical model measuring 30 m × 30 m × 35 m in x, y and z directions respectively was constructed using FLAC^{3D} to simulate the roadway development and the assessment of coal and gas outburst potential at each stage of roadway development. As illustrated in Fig. 5, the model included the coal layer and surrounding strata around a developing roadway without covering the whole longwall panel in the coal seam. The model depth varied from -1,030 to -940 m. The coal seam modelled was located at 1,000 m depth below ground level with a thickness of 3 m. This seam was overlain by a 6 m thick sandstone roof, and underlain by a 16 m thick mudstone floor. The sandstone layer was further underlain by a mudstone layer of 10 m in thickness. A 6 m × 11 m × 3 m outburst prone zone, represented by a much lower coal fracture toughness in the model, was placed in the coal seam 10 m ahead of the roadway, which is developed by progressive excavation steps. The

dimension of the elements in the model is 1 m. The elements in the outburst prone zone were refined down to 0.1 m in each direction to better represent the gas pressure evolution and mechanical behaviour in response to roadway development.

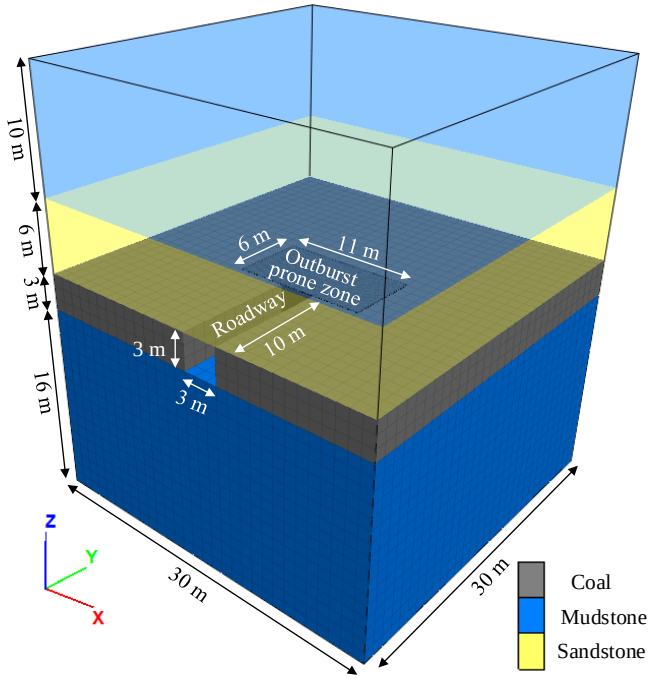

Fig. 5. General stratigraphy and model geometry of roadway development in the modelled coal seam.

Elastic constitutive model was used for all geological structures. The failure of mudstone and sandstone is not considered in this model, and fracture toughness was only assigned to coal formations. Langmuir volume and Langmuir pressure for the coal seam were obtained from the 45°C high pressure adsorption isotherms measured using coal samples collected from the same coal seam. The thickness h of desorption zones around fractures was taken as $a/100$. The outburst prone zone had the same physical, elastic and reservoir properties as the coal seam and a fracture toughness of a quarter of that of the coal seam (fracture toughness of 0.05 MPa·m$^{1/2}$). Physical, rock mechanical and reservoir properties used for geological structures in the model are summarised in Table 1.

The *in situ* vertical stress in the model was induced by the overburden weight (using a density of 2,360 kg/m^3), and the horizontal stresses were estimated by the Poisson's effect under gravity loading of the overburden. The vertical and horizontal stresses at 1,000 m depth were σ_v = 23.13 MPa, and $\sigma_H = \sigma_h$ = 9.45 MPa, respectively. The boundary conditions of the model were such that it was laterally confined and fixed at the base. The saturation gas pressure in the virgin coal seam was taken as 3 MPa.

During geomechanical modelling, a total of five roadway development steps, each representing the removal of a 2 m length of coal, were modelled until the roadway reached the outburst prone zone. The timestep for mechanical calculation was automatically determined based on the minimum eigenperiod of model elements, while the timestep for the calculation of gas-driven fracture behaviour was set to 1 s. The physical time to be modelled after each roadway development step was 360 s in the model.

5. RESULTS AND ANALYSIS

Fig. 6 presents a plan view of the evolution of intra-fracture gas pressure distribution 360 s after each roadway development step. As can be seen, the intra-fracture gas pressure is relieved within a 2 m wide zone ahead of the development face due to mining-induced stresses, but no coal failure is induced during this first four roadway development steps. As the development heading reaches the outburst prone zone in the fifth step, a coal and gas outburst, which spreads within the outburst prone zone, is initiated, whereby the coal elements are expulsed from the seam and a steep gas pressure gradient forms at the outburst front (Fig. 6e).

Fig. 7 illustrates how the outburst progresses from the exposed working face into the outburst prone zone. It can

Table 1 Model parameters used in the numerical model.

Model parameters	Unit	Coal	Mudstone	Sandstone
Physical properties				
Density	kg/m^3	1290	2360	2360
Rock mechanical properties				
Bulk modulus K	GPa	1.26	6.04	8.00
Shear modulus G	GPa	0.60	3.45	3.70
Fracture toughness K_{Ic}	MPa·m$^{1/2}$	0.20	-	-
Adsorption properties				
Langmuir volume V_L	m^3/kg	0.015	-	-
Langmuir pressure p_L	MPa	1.7	-	-
Diffusivity κ	min^{-1}	7.51×10^{-4}	-	-
Fracture attributes				
Radius a_0	m	0.001	-	-

be seen that the coal outburst modelled forms a dome-shaped cavity, which is quite common in field observations (Shepherd *et al.*, 1981). Expulsion of coal at the working face causes the subsequent ejection of neighbouring coal elements by aggravating the release of *in situ* stress and facilitating gas desorption-driven fracture opening and propagation. This results in an accelerated growth of the ejected volume of coal over time. In this perspective, a coal and gas outburst represents a domino effect-type failure, which would proceed continuously given that coal properties, stress conditions and gas pressure remain the same. As illustrated in Fig. 8, the expansion of the outburst zone follows the same pattern as that represented by the onset of gas desorption from the coal elements.

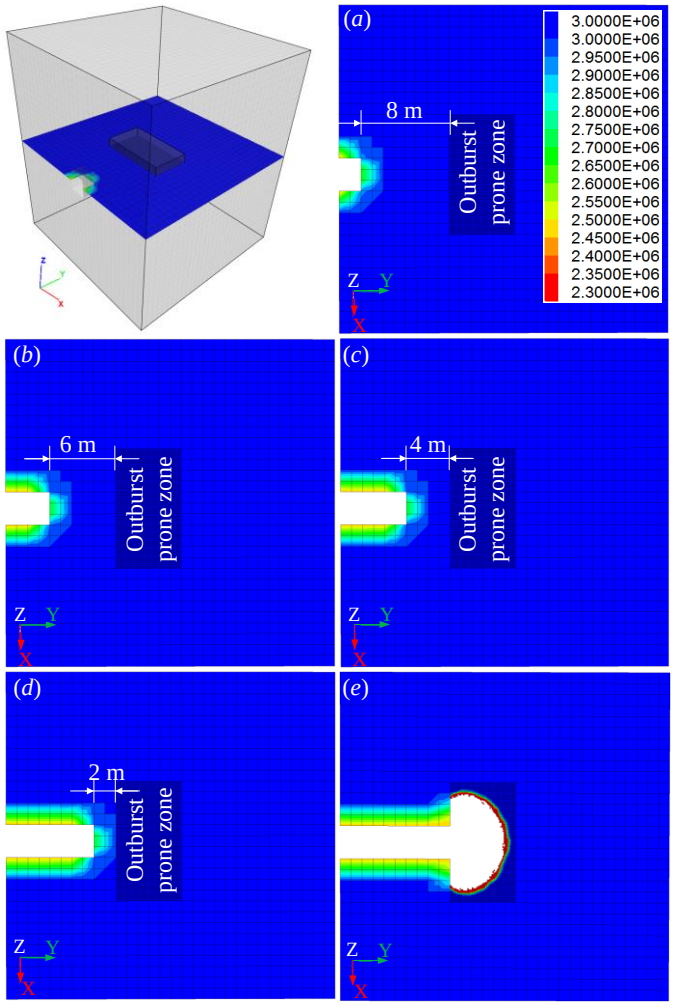

Fig. 6. Intra-fracture gas pressure distribution caused by gas desorption after each roadway development step (Unit: Pa).

Fig. 9 illustrates the distribution of minor principal stress ahead of the development heading when the outburst is initiated. In order to monitor the evolution of minor principal stress and intra-fracture gas pressure, a trace line was drawn from the centroid of the working face in the direction of roadway development, and five measurement points with a spacing of 1 m were assigned along the trace line (Fig. 9). Fig. 10 illustrates the gas pressure variation associated with fracture behaviour in the proximity of the development face during the initiation stage of the outburst. Intra-fracture gas pressure first drops drastically to a value not lower than σ_{min}, and then experiences a gentle increase, followed by a gradual decline, corresponding to three stages of the fracture behaviour, namely fracture opening, expansion and propagation. It is noted that even for coal and gas outburst prone areas, a certain amount of time delay is needed for the intra-fracture gas pressure to build up before it reaches a threshold value to initiate fracture propagation. In this model, fractures located closest to the development face begin to propagate at 11 s and lead to the failure of the host element at 20 s after exposure of the outburst prone zone. This provides an explanation for the short time delay observed before coal and gas outbursts in the field, which ranges from several to tens of minutes after exposure to an outburst prone zone or being initiated by a dynamic disturbance, such as shotfiring (Hargraves, 1980).

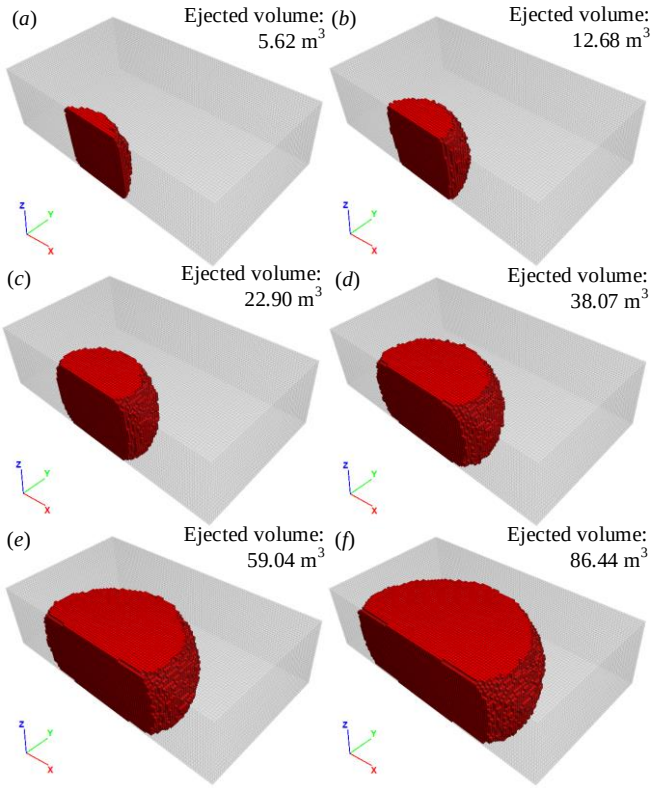

Fig. 7. Extension of the coal outburst zone over time: (a) 60 s, (b) 120 s, (c) 180 s, (d) 240 s, (e) 300 s and (f) 360 s after reaching the outburst prone zone.

Fig. 11 illustrates minor principal stress, intra-fracture gas pressure and effective stress profiles in the outburst prone zone during the development of the outburst. Although the initial gas pressure is much lower than the *in situ* minor principal stress, positive effective stress exists in a localised thin layer at the outburst front, which ensures that the outburst propagates steadily into the outburst prone zone. Fig. 12 plots minor principal stress and intra-

fracture gas pressure variations over time at different monitoring points. It can be seen that minor principal stresses gradually decrease as the development face approaches. When it drops below the initial gas pressure, the intra-fracture effective stress becomes positive, which leads to fracture expansion and in turn influences the intra-fracture gas pressure. It should be noted that intra-fracture gas pressure is always larger than the minor principal stress of the host element so as to sustain the fracture volume after the fracture opens.

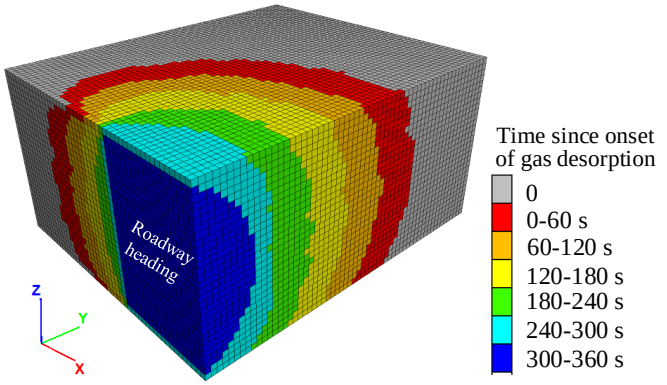

Fig. 8. Time since fracture expansion begins and gas desorption from coal elements is initiated (only the left half of the outburst prone zone is shown).

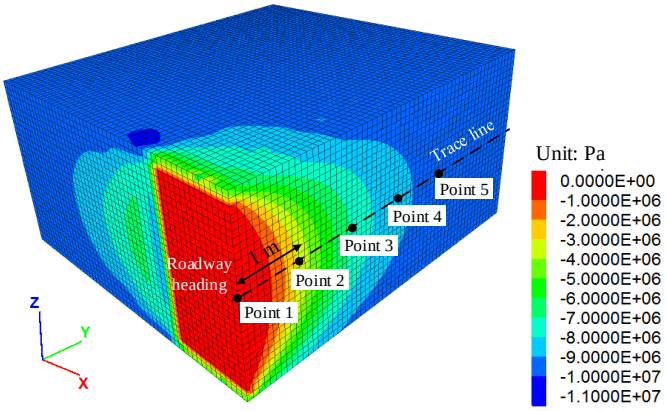

Fig. 9. Minor principal stress contours as the development face reaches the outburst prone zone (only the left half of the outburst prone zone is shown).

6. CONCLUDING REMARKS

Coal and gas outbursts are characterised by a succession of ejection of coal fragments as a result of rapid fracture propagation. In the current research, a theoretical model based on fracture mechanics and adsorption kinetics was developed to describe the behaviour of gas-containing fractures parallel to a working face, which involves opening first, then expansion and finally the rapid propagation stages under excavation unloading conditions. The fracture opening is driven by the effective stress inside the fracture, while the fracture expansion and rapid propagation is propelled by the pressure build-up of desorbed gas in the vicinity of the fracture.

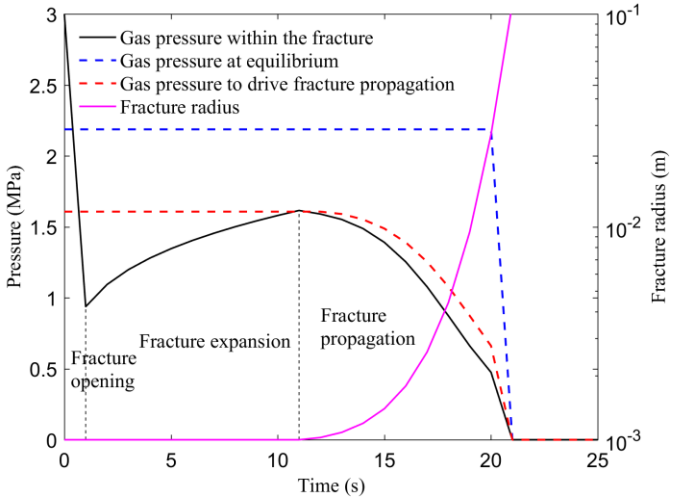

Fig. 10. Evolution of intra-fracture gas pressure and associated fracture behaviour at measurement point 1.

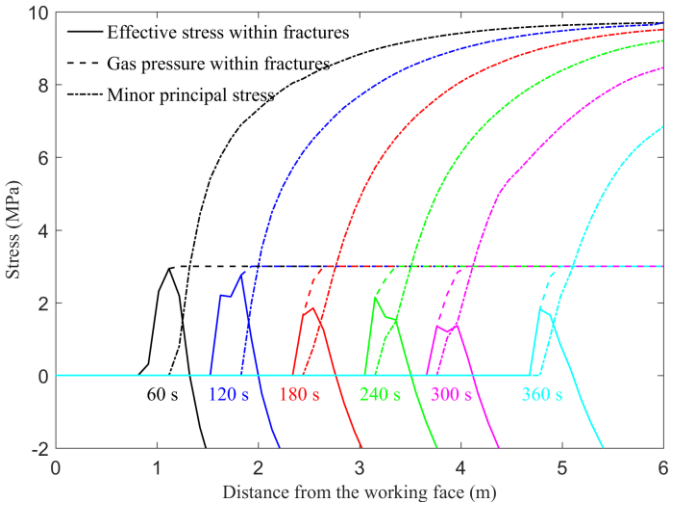

Fig. 11. Minor principal stress, intra-fracture gas pressure and effective stress profiles along the central trace line at different times after the onset of the outburst.

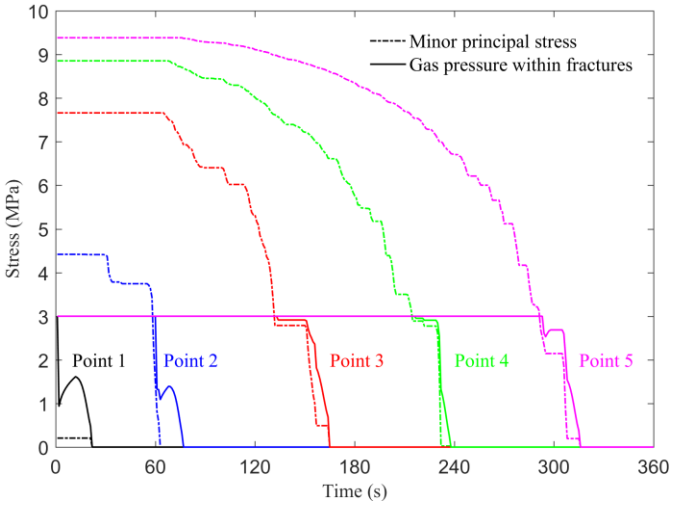

Fig. 12. Minor principal stresses and intra-fracture gas pressures over time at different monitoring points after the onset of the outburst.

The theoretical model developed was implemented in the advanced geomechanical software FLAC3D to simulate coal and gas outbursts. A 3D continuum geomechanical model was constructed to model roadway development towards an outburst prone zone in a coal seam sandwiched between rock layers using field data from a Colliery in Poland. A system of gas-containing fractures oriented parallel to the development face was distributed uniformly throughout the model domain of the coal formation. The numerically implemented model was applied to simulate a coal and gas outburst when the outburst prone zone was reached. Fracture behaviour with response to variations in gas pressure and stress state, and associated failure of host elements with reference to the stress intensity factor of embedded fractures were analysed sequentially at each roadway development step.

The model results have shown that coal and gas outbursts can be considered as a domino effect-type failure triggered by excavation unloading and propelled by gas desorption driven fracture propagation. The coal ejection manifests itself as layer-by-layer breakage, eventually leading to a domed-shape erupted zone. Furthermore, the delayed occurrence of coal and gas outbursts, especially after sudden exposure of soft coal materials or after excitations due to dynamic disturbances, may be associated with the gas desorption behaviour.

ACKNOWLEDGEMENTS

This research was carried out as part of the European Commission Research Fund for Coal and Steel (RFCS) funded project "Monitoring, Assessment, Prevention and Mitigation of Rock Burst and Gas Outburst Hazards in Coal Mines, MapROC", Grant No: RFCR-CT-2015-00005. The first author acknowledges the UK Engineering and Physical Sciences Research Council (EPSRC) scholarship awarded by the Faculty of Engineering at Imperial College London.

REFERENCES

Alekseev, A.D., N.V. Nedodsev, G.P. Starikov. 1980. Fracture of gas-saturated coal under volumetric state of stress in the course of unloading: modelling of outbursts of coal and gas. In: *Institute for Problems in Mechanics of the Russian Academy of Sciences, Moscow*, 139.

Anders, M.H., S.E. Laubach, C.H. Scholz. 2014. Microfractures: A review. *J. Struct. Geol.* 69, 377–394.

Cao, W., J.Q. Shi, S. Durucan, G. Si, A. Korre. 2017. Modelling the Influence of Heterogeneity on Microseismic Characteristics in Longwall Coal Mining. In *51st US Rock Mechanics/Geomechanics Symposium. American Rock Mechanics Association*.

Cao, W., X. Li, M. Tao, Z. Zhou. 2016. Vibrations induced by high initial stress release during underground excavations. *Tunn. Undergr. Sp. Technol.* 53, 78–95.

Chen, K.P. 2011. A new mechanistic model for prediction of instantaneous coal outbursts - Dedicated to the memory of Prof. Daniel D. Joseph. *Int. J. Coal Geol*. 87, 72–79.

Crank, J. 1979. *The mathematics of diffusion*. Oxford University press.

Dyskin, A.V., L.N. Germanovich. 1993. Model of rockburst caused by cracks growing near free surface. In *Rockbursts and Seismicity in Mines*, 169–175.

Farmer, I.W., F.D. Pooley. 1967. A hypothesis to explain the occurrence of outbursts in coal, based on a study of west wales outburst coal. *Int. J. Rock Mech. Min. Sci. Geomech. Abstr.* 4: 189–193.

Feldman, E.P., N.A. Kalugina, T.N. Meln'ik. 2017. Role of unloading and filtration of gas in the development of main cracks in coal seams. *J. Appl. Mech. Tech. Phys.* 58: 155–164.

Hargraves, A.J. 1980. A review of instantaneous outburst data. In: *Proceedings of the Occurrence, Prediction and Control of Outbursts in Coal Mines, Melbourne*, 1–8. The Australian Institute of Mining and Metallurgy.

Langmuir, I. 1918. The adsorption of gases on plane surfaces of glass, mica and platinum. *J. Am. Chem. Soc*. 40: 1361–1403.

Li, X., W. Cao, M. Tao, Z. Zhou, Z. Chen. 2016. Influence of unloading disturbance on adjacent tunnels. *Int. J. Rock Mech. Min. Sci*. 84: 10–24.

Li, X., W. Cao, Z. Zhou, Y. Zou. 2014. Influence of stress path on excavation unloading response. *Tunn. Undergr. Sp. Technol*. 42: 237–246.

Linkov, A.M. 1996. Rockbursts and the instability of rock masses. *Int. J. rock Mech. Min. Sci. Geomech. Abstr*. 33: 727–732.

Odintsev, V.N. 1997. Sudden outburst of coal and gas—failure of natural coal as a solution of methane in a solid substance. *J. Min. Sci*. 33: 508–516.

Rudajev, V., R. Teisseyre, J. Kozak, J. Sileny, 1986. Possible Mechanism of Rockbursts in Coal-Mines. *Pure Appl. Geophys. Pageoph.* 124: 841.

Sack, R.A. 1946. Extension of Griffith's theory of rupture to three dimensions. *Proc. Phys. Soc.* 58: 729–736.

Shepherd, J., L.K. Rixon, L. Griffiths. 1981. Outbursts and geological structures in coal mines: A review. *Int. J. Rock Mech. Min. Sci.* 18: 267–283.

Smith, D., F. Williams. 1984. Diffusional effects in the recovery of methane from coalbeds. *Soc. Pet. Eng. J.* 529–535.

Sneddon, I.N. 1946. The distribution of stress in the neighbourhood of a flat elliptical crack in an elastic solid. In: *Proc. R. Soc, London*, A-187: 229–260.

Zhao, W., Y. Cheng, H. Jiang, K. Jin, H. Wang, L. Wang. 2016. Role of the rapid gas desorption of coal powders in the development stage of outbursts. *J. Nat. Gas Sci. Eng.* 28: 491–501.